Saudi Pharmaceutical Journal 29 (2021) 576–585

Contents lists available at ScienceDirect

Saudi Pharmaceutical Journal

journal homepage: www.sciencedirect.com

Original article

Fluconazole nanoparticles prepared by antisolvent precipitation technique: Physicochemical, *in vitro*, *ex vivo* and *in vivo* ocular evaluation

Amal El Sayeh F. Abou El Ela [a,b,*], Mohamed Abbas Ibrahim [a,c,*], Yara Alqahtani [a], Aliyah Almomen [d], Fadilah Sfouq Aleanizy [a]

[a] Department of Pharmaceutics, College of Pharmacy, King Saud University, Riyadh, Saudi Arabia
[b] Department of Pharmaceutics, College of Pharmacy, Assiut University, 71526 Assiut, Egypt
[c] Department of Pharmaceutics and Industrial Pharmacy, College of Pharmacy, Al-Azhar University, Assiut, Egypt
[d] Department of Pharmaceutical Chemistry, College of Pharmacy, King Saud University, Riyadh, Saudi Arabia

ARTICLE INFO

Article history:
Received 21 October 2020
Accepted 13 April 2021
Available online 23 April 2021

Keywords:
Nanonization
Antisolvent precipitation nanonization
Stabilizers
Fluconazole
Ocular delivery

ABSTRACT

The goal of this research was to prepare and characterize nanonized particles of the antifungal drug, fluconazole (FLZ) using antisolvent precipitation nanonization technique to improve its ocular permeation. The impact of various concentrations of different stabilizers, namely Pluronic F-127 (PL F 127), Kollicoat IR (KL), hydroxypropyl methylcellulose E3 (HPMC), xanthan gum (XG), polyvinyl pyrrolidone K30 (PVP), and sodium lauryl sulfate (SLS) upon the resulting nanoparticles was investigated. Additionally, the *ex vivo* release of the FLZ nanonized particles from ophthalmic gel bases was studied by using goat cornea, and the ocular pharmacokinetics of appropriate ophthalmic gel base containing optimized drug nanoparticle formula compared to the untreated drug were studied in rabbits. FLZ nanoparticles were successfully prepared with different concentrations of stabilizers. However, the effects of these stabilizers on nanoparticle size and zeta potential values varied according to the concentration and type of stabilizer used. Based on differential scanning calorimetry, the drug was in its amorphous state in the tested nanoparticle formulations. The results of *ex vivo* ocular diffusion of the FLZ nanoparticle gel formulations revealed an improvement compared to that with the FLZ untreated gel. Nanoparticle formula (F3) prepared by using 5% PL F127 showed small particle size (352 ± 6.1 nm) with zeta potential value of −18.3 mV with highest *ex vivo* release rate from goat cornea (100% after 6 h). Moreover, the $AUC_{0\text{-}8h}$ from ocular application of FLZ from sodium alginate gel containing nanoparticle formula F3 was 1.4-fold higher than that after its administration in the untreated formula. Based on our findings, the ophthalmic gel formulations containing FLZ nanoparticles enhanced drug corneal permeation and improved the ocular pharmacokinetic parameters.

1. Introduction

Recently, abundant nanonization strategies have been advanced to enhance the bioavailability and dissolution rates of numerous drugs with poor solubility in water. Some of these approaches involve altering the crystallinity of the drug, developing new nanomaterials that can act as drug carriers to attain controlled release, and enlarging the surface area to volume ratios of drug powders (Junghanns and Müller, 2008; Marcato and Durán, 2008) Nanonization can result in enriched drug solubility and pharmacokinetics and might decline systemic side-effects (Chen et al, 2011). In the earlier period, several drug nanoformulations have been clinically accepted or are beneath medical study (Junghanns and Müller, 2008; Marcato and Durán, 2008). The development of nanoformulation technologies, recent pharmaceutical constituents, and quality control have been the attention in research to improve the outcome characters while diminishing production charges. New technological developments and unmet medical requests offer a meaningful pushing power for study and advance of nanonization approaches (Chen et al, 2011).

* Corresponding authors at: Department of Pharmaceutics, College of Pharmacy, King Saud University, Saudi Arabia.
E-mail address: mhamoudah@ksu.edu.sa (M. Abbas Ibrahim).

Peer review under responsibility of King Saud University.

Production and hosting by Elsevier

https://doi.org/10.1016/j.jsps.2021.04.018
1319-0164/

A reduction in particle size leads to an increase in surface area and surface energy, which might induce particle agglomeration. Particles be susceptible to agglomerate as a consequence of the decrease in surface energy required to rebalance the formula. This agglomeration can initiate crystal growth. Therefore, to overcome this issue, it is suggested that a stabilizer, which can inhibit particle agglomeration, be added (Gao et al, 2008; Van Eerdenbrugh et al, 2008).

Stabilizers perform an essential part in the preparation and maintenance of nanoparticles. The high surface energy of nanosized particles can lead to the agglomeration or aggregation of drug crystals in the absence of an appropriate stabilizer. The main functions of a stabilizer include the thorough wetting of drug particles, the prevention of Ostwald's ripening (Paun and Tank, 2012) and the agglomeration of nanosuspension to provide a physically stable formulation with steric or ionic barriers. The type and quantity of the stabilizer have a substantial influence on the physical stability and *in vivo* performance of the nanosuspension (Keck and Müller, 2006; Merisko-Liversidge et al, 2003).

Fluconazole (FLZ) is a solid antifungal that belongs to triazoles that generally acts by inhibiting 14-αsterol demethylase which converts lanosterol to ergosterol to remove lanosterol from the 14α-methyl group (Behrens-Baumann et al., 1990).

As systems have a short contact time with the ocular mucosa, this serves as the major limitation. However, this can be prolonged via modified formulations such as gel bases, inserts, and implants (Hornof et al, 2005). The lipophilic drugs, in this case, remained in the corneal epithelium and were slowly released to the cornea inner layers, followed by the anterior chamber (Wadhwa et al, 2009).

The most familiar administration route for the treatment of diseases of the anterior segment of the eye is the ocular drug delivery. <10% bioavailability is attained with topical ocular drug application although this delivery route is effortless, suitable, and painless. This little bioavailability is ascribed to ocular protecting biological barriers, such as the impermeable corneal epithelium, which represents a barrier for drug permeation into the eye. Owing to lacrimal secretion and nasolacrimal drainage, fast removal of the instilled ophthalmic drug solution happens from the precorneal region. Consequently, repeated instillation of ophthalmic solutions is essential to get the necessary therapeutic effects. Therefore, effective topical liberation of drugs to ocular tissues is a challenge for formulation scientists. Innovative technologies were progressed to increase the bioavailability of ophthalmic drugs. Examples of the functional technologies include mucoadhesive systems, in situ gelling systems, microparticulate and nanoparticle systems, microemulsions, vesicular systems, implants, prodrugs, penetration enhancers, and dendrimers (Sayed et al, 2015; Zimmer and Kreuter, 1995).

Numerous formulation methodologies have been tried to enhance FLZ ocular efficacy. For example, FLZ ocular liposomal formulation of was effective in eradicating Candida albicans infection of the rabbit cornea in comparison to the FLZ solution (Habib et al, 2010). In addition, Gonjari et al. showed that in situ forming gel containing FLZ revealed an improved corneal permeation of FLZ, and it was superior to the drug aqueous solution. (Gonjari et al, 2009). Also, Abdellatif et al (Abdellatif et al, 2019) prepared FLZ nanoparticles coated with polyethylene glycol using antisolvent precipitation method. They found that the drug antifungal activity was better from hydrogel containing PEG-coated nanoparticles compared to same hydrogel formulation containing untreated FLZ. However, these investigations were based on the formulation of polymeric nanoparticles containing FLZ, and no study discussed the ocular efficacy of nanonized FLZ particles.

The present work aimed to formulate FLZ nanoparticles by using antisolvent precipitation technique to increase the drug ocular penetration and to improve its ophthalmic antifungal efficiency. The influence of utilizing numerous kinds and concentrations of stabilizers in the method on the resultant nanoparticles was examined. The *in vitro* and *ex vivo* release of the FLZ nanonized particles from the cellophane membrane and goat cornea, in addition to the ocular pharmacokinetics of suitable ophthalmic gel bases in rabbits were also evaluated.

2. Materials and methods

2.1. Materials

FLZ was obtained as a gift from Aljazerah Pharmaceutical Company (Riyadh, Saudi Arabia). Hydroxypropyl methylcellulose low viscosity; viscosity of ~ 3 cP for 2% aqueous solution, MWT ~ 20,000 Da; (HPMC LV grade E3) was gained from Dow Chemical Co. (Midland, MI, USA). Kollicoat IR (KL) was obtained from BASF (Ludwigshafen, Germany). Pluronic F-127 (PL F127) was purchased from C.H. (Erbesloh, Krefeld, Germany). Xanthan gum (XG) was purchased from Sigma Chemical Co. (MO, USA). Polyvinyl pyrrolidone K30 (PVP; molecular weight 30,000 Da) was purchased from ISP Technologies, Inc. (NJ, USA). SLS was bought from Fisher Scientific International, Inc. (NH, USA). Carbopol 934 was obtained from Goodrich Chemical Co. (Poole, England). Sodium alginate was purchased from Sigma Chemical Co. (MO, USA). Standard dialysis cellophane membrane, molecular weight cut off ≈ 14,000 (Sigma chemical Co., MO, USA).The acetonitrile (HPLC–gradient) was purchased from Panreac (Madrid, Spain). Formic acid was purchased from Fisher Scientific (MA, USA).

2.2. Preparation of the nanoparticles by the antisolvent precipitation method

An exactly weighed quantity of 100 mg of FLZ was dissolved in 3 mL of dichloromethane. Thereafter, by using a syringe, the drug was dropped into distilled water (20 mL) containing the stabilizer (0.5, 1, 5 w/v %) under magnetic stirrer at 1000 rpm for 4 h until the solvent was completely evaporated, thereby resulting in supersaturation of the FLZ in solution and nanoparticle formation. The prepared FLZ nanosuspensions were frozen at −30 °C and finally dried with a freeze-dryer (Martin Christ, Osterode, Germany) at −40 °C (Ibrahim et al., 2019).

2.3. Evaluation of the prepared FLZ nanoparticles

2.3.1. Determination of particle size and zeta potential

Photon correlation spectroscopy (PCS) using Zetasizer (Nano ZS, Malvern Instruments, UK) at room temperature was applied to determine the mean particle size and zeta potential of the freeze-dried nanoparticles. The samples were placed in an electrophoretic cell after adequately diluted with deionized water (1: 1000). All investigations were performed in triplicate.

2.3.2. Determination of FLZ content in lyophilized nanoparticles

Accurately weighed 5 mg sample was dissolved in 5 mL methanol, transferred to 50 mL volumetric flask. The volume was made up using phosphate buffer pH 6.8. The absorbances at 260 nm were measured by using UV spectrophotometer, Biochrom Libra S22 (Cambridge, England), and the drug content was calculated consequently. The experiment was performed in triplicate.

2.3.3. Differential scanning calorimetry (DSC)

The extent of the crystallinity of the drug in its nanoparticles prepared by different stabilizers was assessed by DSC studies.

The DSC thermograms of the bulk FLZ powder and the lyophilized nanosuspension compared to the related drug physical mixtures (FLZ: stabilizing polymer in 1: 1 ratio) with the tested considered stabilizers were drawn with a DSC 4000 (Perkin Elmer Instruments, USA) at a temperature between 30 and 200 °C and a heating rate of 10 °C/min with a nitrogen supply of 50.0 mL/min.

2.3.4. X-ray powder diffraction (XRPD)

To determine the crystallinity of pure drugs in the nanoparticles, XRPD of pure drugs and selected nanoparticle samples were evaluated by Ultima IV diffractometer (Rigaku Inc. Tokyo, Japan) over the 3 – 60° 2θ range at a scan speed of 1°/min. The tube anode was Cu with Ka = 0.1540562 nm mono chromatized with a graphite crystal (Rigaku Inc. Tokyo, Japan). The pattern was collected at 40 kV of tube voltage and 40 mA of tube current in step scan mode (step size 0.02°, counting time 1 s per step).

2.3.5. Solubility study

Saturation solubility studies of the untreated drug and the selected lyophilized nanoparticles were carried out. Briefly, FLZ nanoparticle equal to 10 mg of drug was weighed and individually introduced into a stoppered conical flask including 5 mL of phosphate buffer (pH 6.8). The flasks were preserved in a water bath shaker (37 °C ± 0.5) at 100 rpm for 72 h. Thereafter, 0.5 mL samples were withdrawn and filtered through a 0.22 μm Millipore filter. A 100 μL aliquot of each filtrate was diluted properly with phosphate buffer (pH 6.8) and evaluated by means of a UV spectrophotometer at 260 nm. Each experiment was carried out in triplicate.

2.4. Formulation of FLZ nanoparticles in ophthalmic gel bases

The ophthalmic gel containing 0.5% w/w of untreated FLZ or selected drug nanoparticle formula equivalent to 0.5% w/w of FLZ was prepared using two gelling polymers, carbopol and sodium alginate. One nanoparticle formula was selected from each stabilizer based on small particle size and high zeta potential. The gel was prepared using carbopol 934 (1% w/w) and sodium alginate (3% w/w). Accurately weighted amount of carbopol 934 powder was sprinkled into distilled water beneath regular mixing by a magnetic stirrer at 1000 rpm until carbopol dispersion was achieved. Subsequently, untreated FLZ (F0) or drug nanoparticle formulation holding 5 mg of drug (equivalent to 0.5% w/w of the total gel weight) was added at the similar agitating situation. The mixture was neutralized using triethanolamine (0.5% w/w). The sodium alginate gel was prepared by adding an appropriate amount of the polymer to water at 40 °C under constant stirring with a magnetic stirrer at 1000 rpm until complete dissolution was achieved. Subsequently, the nanoparticle drug formulation was added until complete dispersal was obtained (Abou el Ela and, El Khatib, 2014).

2.4.1. Visual examination

The FLZ nanoparticle-loaded gel bases were evaluated to determine their homogeneity, color, and the presence of lumps via visual examination.

2.4.2. pH measurement

The pH of all gel formulations was determined by dipping the pH-electrode of a digital pH meter (Mettler Toledo, Switzerland) in the gel formulations. The mean of the three outcomes was documented.

2.4.3. Rheological study

The viscosity of the various gel preparations was determined at 25 °C using cone and plate viscometer with spindle 25 (Brookfield Engineering Laboratories, model HADV-II, Middleboro, MA). Accurately weighted 0.5 g of the formulation was placed on a plate and allowed to reach equilibrium. The shear rate ranged from 10 to 60 s^{-1} with 2 min between every 2 consecutive speeds. The viscosity values were determined from the obtained rheograms. The whole measurements were operated in triplicate (Abou el Ela and, El Khatib, 2014).

2.4.4. Transmission electron microscopy (TEM)

The morphology and size of the nanoparticles were evaluate applying TEM. The nanoparticle suspension of the selected formula and the nanoparticle-containing gel of the selected formula with sodium alginate was dropped onto carbon-coated copper grids for observation with the TEM jem-1400 (JEOL LTD, Tokyo, Japan). An imaging software was used for image capture and analysis.

2.4.5. In vitro drug release study

The *in vitro* release studies of FLZ gel formulations containing untraded drug or selected nanoparticle formulation was performed in 12 mL of the buffered solution (pH 7.4) at 37 ± 0.5 °C and 100 rpm using the Franz diffusion method (Logan instruments, NJ, USA). A semipermeable membrane from Sigma Chem. Co. (USA) with a molecular cut-off of 14,000 Da was employed herein. An accurately weighted 1 g of ophthalmic gel containing 5 mg FLZ was applied to the donner compartment side of the membrane. Samples of 1 mL each were removed at several time intervals of 1, 2, 4, and 6 h, and quantified. All samples were filtered through a 0.22 μm pore size cellulose membrane filter and analyzed at λ_{max} of 260 nm with a spectrophotometer (Biochrom Libra S22, Cambridge, England). Each experiment was carried out in triplicate. Different Kinetic models were used to evaluate the *in vitro* release data.

2.4.6. Ex vivo permeation study

The permeation of FLZ across the corneal membrane of the goat cornea from selected ophthalmic gel containing drug nanoparticles formula (showed highest release rate from *in vitro* drug release study) was studied, and compared to gel containing untreated drug formulation. Briefly, whole eyeballs of goats were obtained from a slaughterhouse and transferred to the laboratory under cold environments in normal saline kept at 4 °C (Pathak et al., 2013). The cornea was thoroughly detached along with 5–6 mm of surrounding scleral tissue and cleaned with cold saline. The washed corneas were maintained in cold recently prepared solutions of tear buffer (phosphate buffer saline; pH 7.4). The experiment was carried out in Franz vertical diffusion cell. One g of the different nanoparticle gel formulations containing 0.5% w/w of FLZ was placed on the corneal membrane (0.9 cm) of the goat by using the diffusion cell at a pH 7.4. Precaution was trained to confirm that the corneal membrane slightly touched the receptor medium surface. The entire system was kept at 37 ± 0.5 °C and stirred at 100 rpm. Aliquots of 1 mL were withdrawn at different time intervals of 1, 2, 4, 6, and 8 h and exchanged with an equivalent quantity of fresh buffer solution. All samples were filtered through a 0.22 μm pore size Millipore membrane filter and assayed at λ_{max} of 260 nm using a UV spectrophotometer (Cambridge, England). All experiments were carried out in triplicate.

2.5. Ocular pharmacokinetics

The FLZ nanoparticle sodium alginate gel (F3) was selected to evaluate the pharmacokinetic parameters of FLZ relative to the untreated FLZ nanoparticle sodium alginate gel (F0). F3 was selected according to its *in vitro* and *ex vivo* release profile, which revealed its significantly higher drug release rate ($P < 0.05$) relative to other formulations. Moreover, complete drug release was attained within 6 h in the *in vitro* experiment. From the *ex vivo* study, the cumulative amount of FLZ permeation was 621 ± 4.9 μg/cm^2.

2.5.1. Animal handling

Thirty-three Albino rabbits (weight 2 to 2.5 kg) were gained from King Abdulaziz City for Science and Technology (KACST). The investigation was approved by the Ethical Committee (Ethics reference No: SE-19–110) of the Experimental Animal Care Unit. The experimental protocol aligned with the Guide of the National Institutes of Health (NIH) for the Care and Use of Laboratory Animals. Animals were individually housed in a temperature-controlled animal facility, with a 12 h light/night cycle. Animals were granted free access to water and food.

2.5.2. Ocular administration

Rabbits were randomly separated into two groups (3 animals per group and 3 animals per time point). One group received 200 mg of sodium alginate gel containing 5 mg of the FLZ nanoparticle (F3) equivalent to 0.5% (w/w) FLZ in the right eye (Pathak et al., 2013). The second group received a similar amount of sodium alginate gel containing untreated FLZ once in the right eye. At predetermined time points (0.5, 2, 4, 6, and 8 h), rabbits were anesthetized with ketamine/xylazine (25/5 mg/kg) and 80 μL of the aqueous humor was withdrawn using a linear probe implanted with a 22-gauge needle. Aqueous humor samples were also withdrawn from control rabbits (n = 3) for comparison. All samples were immediately placed on ice and transferred to a −20 °C freezer for storage until the analysis (El-Kamel, 2002).

2.5.3. Analytical method

The assay was conducted utilizing the Waters Xevo TQ-S UPLC-MS/MS system (Waters, Singapore), with a cooling autosampler and a column oven. The BEH™ Acquity UPLC C18 Column (50 mm*2.1 mm, 1.7μ m) was also employed for the analysis. The mobile phase contained (90/10) acetonitrile/water and 0.1% formic acid and was injected at a flow rate of 0.3 mL/min. Detection was carried out at MRM transition of m/z 307.2 → 238.2 and UV at 260 nm. All data collected in the multi-channel analysis (MCA) were acquired and processed using Mass Lynx™ V 4.1 software with a quanLynx™ V 4.1 program (Waters Corp., Milford, USA). The process was validated for selection, linearity, precision, accuracy, carry over, extraction recovery, and stability prior to the study's initiation as stated by the published assay (Abbasoglu et al, 2001).

Standard solutions containing FLZ at concentrations of 500, 700, 1000, 1500, 2000, and 5000 ng/mL were employed and measured with caffeine as an internal standard (100 ng/mL). The calibration curve was derived by plotting the peak area ratios of FLZ and the internal standard in standard samples against the concentration of FLZ in the aqueous samples using linear regression analysis. The calibration charts between 500 and 5000 ng/mL were establish to be linear, with a regression coefficient (r) > 0.99933.

2.5.4. Aqueous humor sample preparation

To prepare the sample for analysis, the mobile phase was first mixed with caffeine, as an internal standard, at a concentration of 100 ng/mL. The aqueous humor (50 μL) and the mobile phase/caffeine mixture (100 μL) were added to an Eppendorf tube. Subsequently, the mixture was vortexed at 8000 rpm for 15 min at 4 °C. The supernatant was then transferred to a glass screw–capped tube, and 10 μL was injected into the UPLC-MS/MS system.

2.5.5. Pharmacokinetic (PK) analysis

The *trans*-corneal permeated drug concentration of FLZ is presented as mean ± S.D. PK analysis were performed using PK Solver Add-In software. The PK parameters were estimated using the model–independent methods. The elimination rate constant (K) was estimated from a linear regression analysis of the terminal portion from the log-linear aqueous humor concentration–time profile. From the terminal elimination rate constant using the formula: $t_{1/2}$ = 0.693/K the elimination half-life ($t_{1/2}$) was evaluated. The maximum peak drug concentration (C_{max}), and the time to reach maximum concentration (T_{max}) were directly obtained from the aqueous humor-time curve. The area under the curve for each drug concentration–time curve from 0 to 8 h $AUC_{0\text{-}8h}$ was determined using the trapezoidal rule.

2.6. Statistical analysis

Data were analyzed by ANOVA to derive the P-values for the different variables. Fisher's least significant difference (LSD) test was used (in this method, 5.0% risk of calling each pair of means significantly different when the actual difference equal 0) to derive the significant differences between two variables.

3. Results and discussion

3.1. Evaluation of the prepared FLZ nanoparticles

3.1.1. Determination of particle size and zeta potential

Table 1 showed the particle size and zeta potential values of the FLZ nanoparticle formulations stabilized with different stabilizers. The FLZ nanoparticles were successfully prepared by using different concentrations of the stabilizers. However, the effects of these stabilizers on the nanoparticle size and the zeta potential values were found to vary according to the concentrations and types of stabilizers. A nanoparticle formula with each stabilizer was selected for further investigations, including *in vitro* and ex vivo permeation from different corneal gel bases.

It was observed generally from the results obtained that increasing the concentration of stabilizer from 0.5% to 5% caused a decrease in the FLZ nanoparticle sizes. However, this notices was not achieved at 1% stabilizer concertation.

The measured particle sizes of the FLZ nanoparticles stabilized by 0.5%, 1%, and 5% w/v of PL F 127 188.9 ± 3.0 nm, 219.2 ± 7.4 n m and 352 ± 6.1 nm , respectively. Moreover, the PDI values were 0.36–0.41 while the zeta potential values were −17.4 mV, −19.4 mV, and −18.3 mV, respectively. Alshora et al (Alshora et al, 2020) showed PL F-127 concentration showed a slight effect on the size of pioglitazone HCl nanoparticles prepared by wet milling decreased significantly.

Different concentrations of the stabilizer (KL) had pronounced impact on the particles in the FLZ nanoparticles. The drug nanoparticles stabilized by KL showed relative large sizes in all tested stabilizer concentrations, with higher PDI values (about 0.59). For example, the measured particle of the freeze-dried FLZ nanoparticles stabilized by 0.5% KL was 586 ± 7.7 nm, and those stabilized by 5% w/v of KL showed particle size of 553.2 ± 3.6 nm. The measured zeta potential values of the nanoparticles were −30.1 mV, −21.6 mV, and −26.1 mV for F4 (stabilized by 0.5% KL), F5 (stabilized by 1% KL), and F6 (stabilized by 5% KL), respectively.

By determining the impact of HPMC on the size of the produced FLZ nanoparticles, the polymer could produce nanoparticles of small sizes upon using 0.5 and 1% polymeric concentration (624. 3 ± 20.0 to 476.7 ± 19.6 nm) with PDI values ranging from 0.56 to 0.64. Furthermore, the zeta potential values were –22.3 mV and 28.3 mV for the freeze-dried nanoparticles stabilized by 0.5% and 1% HPMC, respectively. Concerning nanoparticles stabilized by highest HPMC concentration (5%), it was difficult to determine particle size or zeta potential value of this disperse due to the highest viscosity and stickiness of the freeze-dried powders. This might be due to the high viscous polymeric concentration that was produced upon using 5% HPMC (Alshora et al, 2018).

According to the findings for the effect of XG on the size of the produced FLZ nanoparticles, similar to the findings with drug

Table 1
Particle size, zeta potential, polydispersity index (PDI) and drug content values of FLZ freeze- dried nanoparticles stabilized by different stabilzers.

Formula	Freeze dried nanoparticle			
	Particle size (nm ± SD)	PDI (±SD)	Zeta potential (mV ± SD)	Drug content (%)
F 1 (PL F 127 0.5%)	188.9 ± 3.0	0.360 ± 0.12	−17.4 ± 1.1	103 ± 0.02
F 2 (PL F 127 1%)	219.2 ± 7.4	0.297 ± 0.05	−19.4 ± 0.06	105.27 ± 0.01
F 3 (PL F 127 5%)	352 ± 6.1	0.411 ± 0.12	−18.3 ± 0.58	97.03 ± 3.04
F 4 (KL 0.5%)	586 ± 7.7	0.586 ± 0.14	−30.1 ± 0.10	92.64 ± 0.20
F 5 (KL 1%)	633.5 ± 19.1	0.590 ± 0.07	−21.6 ± 0.38	89.76 ± 0.10
F 6 (KL 5%)	553.2 ± 3.6	0.583 ± 0.07	−26.1 ± 0.06	89.20 ± 0.60
F 7 (HPMC 0.5%)	624.3 ± 20.0	0. 643 ± 0.19	−22.3 ± 0.06	94.21 ± 0.03
F 8 (HPMC 1%)	476.7 ± 19.6	0.560 ± 0.03	−28.3 ± 0.61	110.84 ± 0.02
F 9 (HPMC 5%)	N/A			
F 10(XG 0.5%)	717.2 ± 6.0	0.742 ± 0.02	−15.7 ± 0.31	113.3 ± 2.00
F 11 (XG 1%)	517.2 ± 9.2	0.542 ± 0.01	−35.8 ± 0.65	113.3 ± 3.00
F 12 (XG 5%)	N/A			
F 13 (PVP 0.5%)	180.4 ± 7.8	0.382 ± 0.04	−24.5 ± 0.47	103.91 ± 6.01
F 14 (PVP 1%)	253 ± 7.7	0.375 ± 0.02	−12.7 ± 0.47	113.73 ± 4.00
F 15 (PVP 5%)	101.5 ± 6.2	0.507 ± 0.06	−18.5 ± 0.15	101.72 ± 7.50
F 16 (SLS 0.5%)	455.8 ± 17.0	0.493 ± 0.05	−53.9 ± 0.21	107.67 ± 6.30
F 17 (SLS 1%)	675.9 ± 5.28	0.777 ± 0.01	−48.4 ± 0.12	87.41 ± 4.02
F 18 (SLS 5%)	160.8 ± 3.60	0.304 ± 0.01	−24.9 ± 0.49	111.11 ± 8.07

nanoparticles stabilized by HPMC, the polymer produced nanoparticles of relatively large sizes. Also, increasing polymer concentration from 0.5% to 1% resulted in reducing nanoparticle size (717. 2 ± 6.0 nm and 517.2 ± 9.2) nm particle sizes were observed for FLZ nanoparticles stabilized by 0.5% and 1% XG, respectively as presented in Table 1, with zeta potential values of −15.7 and −35.8 mV for nanoparticles stabilized by 0.5% and 1% XG, respectively. Previous studies showed that XG enhance the stability of the nanoparticles and nanosuspensions via adsorption to the surface of the iron, thereby providing steric repulsion among the particles and increasing the viscosity of the suspension to ultimately slow the aggregation processes (Xue and Sethi, 2012).

An increase in the PVP concentration from 0.5% to 5% for the FLZ nanoparticles stabilized by different concentrations of PVP, exhibited a pronounced reducing effect on the particles. The determined particle sizes of the FLZ freeze-dried nanoparticles stabilized by 0.5%, 1%, and 5% w/v of PVP were 180.4 ± 7.8 nm, 253 ± 7.7 nm and 101.5 ± 6.2 nm, respectively. The recorded zeta potential values of these freeze-dried nanoparticles were −24.5 mV, −12.7 mV and −18.5 mV, respectively. Alshora et al. (Alshora et al, 2018) observed that increasing PVP concentration from1 to 10%, rosuvastatin calcium nanoparticle sizes were reduced remarkably, and they showed that the optimum stabilizer concentration to achieve small nanoparticle sizes was 5%.

The effect of SLS on the size of the FLZ nanoparticles is displayed in Table 1. Based on our findings, the anionic surfactant produced nanoparticles of the small sizes at higher surfactant concentration (5%), by increasing the surfactant concentration; a noticeable decrease in particle size was detected. The nanoparticles stabilized by the 0.5 and 1% concentrations of SLS (F16 and F17) exhibited particle sizes of 455.8 ± 17.0 nm and 675.9 ± 5.28 nm, respectively and by increasing SLS concentration, FLZ nanoparticle size was reduced to 160.8 ± 3.60 nm.

3.1.2. Determination of FLZ content in lyophilized nanoparticles

Table 1 shows that the FLZ content in the prepared nanoparticles was found in the range of 87.41 ± 4.02 to 113.73 ± 4.00 of the theoretical content.

3.1.3. Differential scanning calorimetry (DSC)

The thermograms in Fig. 1 (A) represent the pure materials, including FLZ, PL F 127, and the FLZ nanoparticles containing three concentrations of PL F 127 (0.5, 1, 5%). The pure drug exhibited an endothermic peak at 140.96 °C, corresponding to its melting point (PL F 127 melting point = 58.93 °C). The DSC scan of the FLZ nanoparticle formulation stabilized by 0.5% of PL F 127 revealed that the drug endothermic peak appeared at its original temperature, but with very low intensity. Conversely, the drug endothermic peak entirely missing in the FLZ nanoparticle formulations stabilized by 1 and 5% of PL F 127. The DSC scans of the FLZ nanoparticles prepared with the three concentrations of KL (0.5, 1, and 5%) compared to the individual components are depicted in Fig. 1(B). The polymer showed a broad and shallow melting endothermic peak at 213.02 °C. DSC scan of the FLZ nanoparticle formulation stabilized by 0.5 and 1% of KL revealed that its drug endothermic peak appeared at its original temperature, but with very low intensity. In contrast, the drug endothermic peak of the FLZ nanoparticle formulations stabilized by 5% KL completely disappeared. The DSC thermograms of the FLZ nanoparticles prepared using the three concentrations of HPMC (0.5, 1, and 5%) are presented in Fig. 1 (C). The drug endothermic peak totally disappeared in the FLZ nanoparticles stabilized by 0.5 and 1% of HPMC. Notably, the FLZ nanoparticle formula stabilized with 5% HPMC was extremely sticky and difficult to process. The DSC thermographs of the FLZ nanoparticles prepared with the two concentrations of XG (0.5 and 1%) are shown in Fig. 1(D). For the FLZ nanoparticles stabilized by 0.5 and 1% of XG the drug endothermic peak was detected at a lesser temperature (139.8 °C), with a decline in its intensity. It is worthy to mention that the FLZ nanoparticle formula stabilized using 5% polymer was extremely sticky and difficult to process, similar to that with 5% HPMC. Fig. 1 (E) shows the DSC thermographs of the FLZ nanoparticles prepared with the three concentrations of PVP (0.5, 1, and 5%) compared relative to the individual components. Due to water evaporation, PVP had a very broad melting endothermic peak around 80 °C. The data acquired from DSC presented that the drug endothermic peak completely disappeared. SLS by 0.5% (F16) and 1% (F17), Fig. 1 F, showed that the drug melting peak slightly shifted to lower temperatures (~138 °C), with very low intensity. In contrast, the drug endothermic peak completely disappeared in the FLZ nanoparticle formulations stabilized by 5% SLS (F18).

The data of DSC scans of the FLZ nanoparticles stabilized by different stabilizers indicated that drug melting peak was disappeared, shifted to lower temperatures or showed low melting intensity, especially at higher stabilizer concentrations. These findings might suggest the decrease of the crystallinity of FLZ in nanoparticle formulations (Ibrahim, 2014).

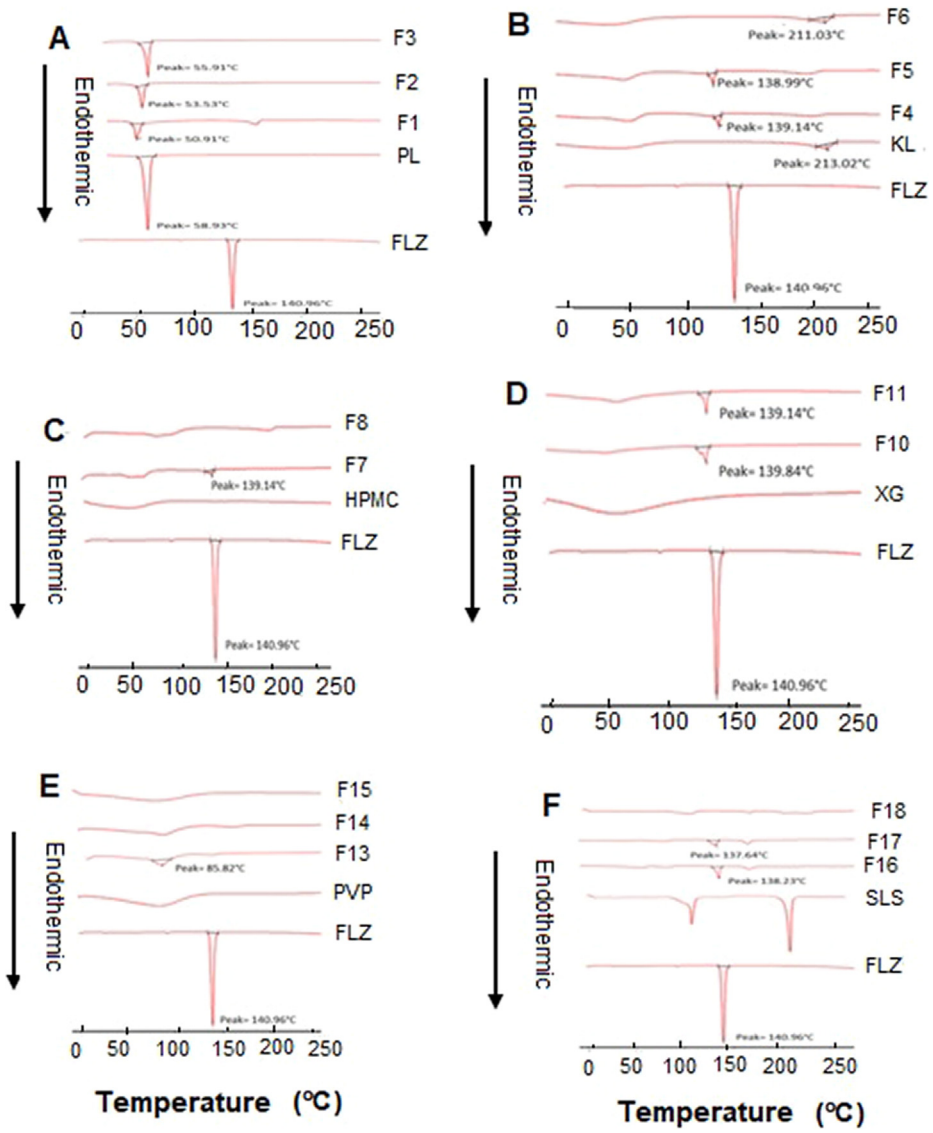

Fig. 1. DSC scan of FLZ nanoparticles stabilized by different stabilizers concentrations compared to the individual components. (a) Pluronic, (b) Kollicoat IR, (c) HPMC, (d) Xanthan gum, (e) PVP and (f) Sodium lauryl sulphate.

3.1.4. X-ray powder diffraction study (XRPD)

To get further evidence on the solid state changes, x-ray diffraction spectra were carried out on FLZ, PL and nanoparticles formulations stabilized by 5% PL F 127 (F3). The presence of numerous distinct peaks in the x-ray diffraction spectrum of FLZ indicates that the drug is present as a crystalline material with characteristic diffraction peaks appearing at diffraction angles of 2q at 5.98 Å, 5.12 Å, 4.53 Å, 3.63 Å, 3.32 Å, 3.05 Å, and 2.85 Å. In addition, PL F 127 copolymer exhibited two characteristic peaks at 19.2, 24.0, Fig. 2. The characteristic diffraction peaks of FLZ nanoparticle formula stabilized by 5%v PL F 127 showed complete disappearance. The obtained data of x-ray studies confirm the data obtained from DSC studies, that confirm that homogenous dispersion of FLZ in PL matrices and the transformation of FLZ to an amorphous or less crystalline form in these nanoparticle formulations (Ibrahim et al. (2019)).

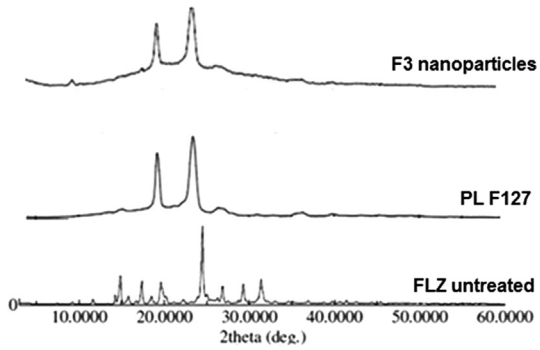

Fig. 2. X-ray powder diffraction spectra of FLZ, PL F 127 and FLZ nanoparticle formula stabilized by 5% PL F 127 (F3).

3.1.5. Solubility study

We determined the aqueous solubility of the FLZ raw material and the selected FLZ nanoparticles stabilized by different stabilizer concentrations at 37 °C The untreated FLZ had an aqueous solubility of 1.2 ± 0.22 mmol/L. The FLZ nanoparticles had significantly enhanced aqueous solubility compared to the untreated drug. The measured drug solubility of FLZ was 2.8 ± 0.808, 2.91 ± 2.521, 3.3 ± 0.332, 4.2 ± 0.180, 6.4 ± 0.323, and 5.9 ± 0.494 mmol/L for

the nanoparticle formulations stabilized by PL F 127 (F3), KL (F4), HPMC (F7), XG (F11), PVP (F13), and SLS (F16), respectively.

A nanoparticle formula was selected (based on high drug solubility, small nanoparticle size) from each stabilizer for further investigations, including *in vitro* and ex vivo permeation from different corneal gel bases. These formulations were F3 (stabilized by 5% PL F 127), F4 (stabilized by 0.5% KL), F7 (stabilized by 0.5% HPMC), F11 (stabilized by 1% XG), F13 (stabilized by 0.5% PVP), and F16 (stabilized by 0.5% SLS).

3.2. Evaluation of the ocular gel bases containing the FLZ nanoparticles

3.2.1. Visual examination

The gel formulations were visually evaluated to derive their appearance, including their homogeneity, color, consistency, and spreadability. The prepared sodium alginate gel appeared transparent yellowish, whereas the gel preparations with sodium alginate were transparent, homogenous viscous. Both gel formulations exhibited a smooth consistency.

3.2.2. pH study

The pH of all gel formulations was in the range, 6.90–7.30. This finding is deemed acceptable to avoid the risk of irritation when applied to the eye.

3.2.3. Rheological study

The viscosity-shear rate profiles of the FLZ nanoparticle gel formulations of carbopol 934 and sodium alginate are presented in Figs. 3 and 4. All gel formulations containing the FLZ nanoparticle had a non-Newtonian pseudoplastic flow behavior (shear thinning systems) at 25 ± 0.5 °C. As the shear rate increased, the normal molecular structure of the gelling material was found to align at its long axes in the direction of flow, thereby decreasing the internal resistance of the material and ultimately, its viscosity (Abou el Ela et al., 2017).

By comparing the viscosity of the FLZ nanoparticle formulations incorporated in carbopol 934 to other formulations using sodium alginate, carbopol 934 produced a higher viscosity than the sodium alginate formulations. This result was obtained for all shear rates from 10 to 60 s^{-1}. At a shear rate of 20 s^{-1}, the viscosity in the carbopol 934 gel formulation was 4.999 ± 0.55 Pa.s compared to the 0. 484 ± 0.11 Pa.s obtained for the sodium alginate gel formulation, F3. The same results were obtained with other shear rates and formulations. By examining the rheology of carbopol 934, The ocular shear rate is an important factor as the ophthalmic blinking shear rate ranges from 4250 – 28,500 s^{-1}; thus, the high viscosity under low shear rate and low viscosity under elevated shear rate situations are usually favored for the viscoelastic fluid (Zaki et al, 2011).

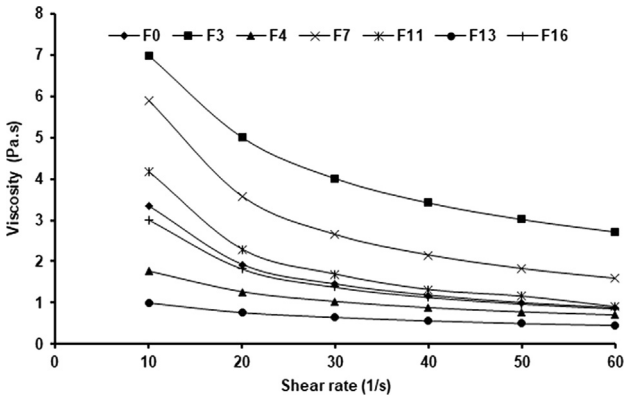

Fig. 3. Viscosity-shear rate profiles of selected carbopol 934 gels containing FLZ nanoparticles (n = 2, mean ± SD).

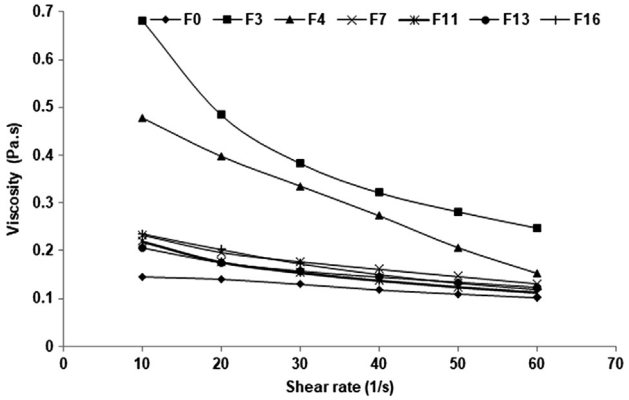

Fig. 4. Viscosity-shear rate profiles of sodium alginate gels containing FLZ nanoparticles (n = 2, mean ± SD).

3.2.4. Transmission electron microscope (TEM)

TEM was employed to confirm the particle size derived by laser scattering spectroscopy. The FLZ appeared dark and spherical against the bright background as shown in Fig. 5 (A). TEM images also showed that the particle sizes were in the nanosize range. However, the particle size of the F3 nanoparticle measured with

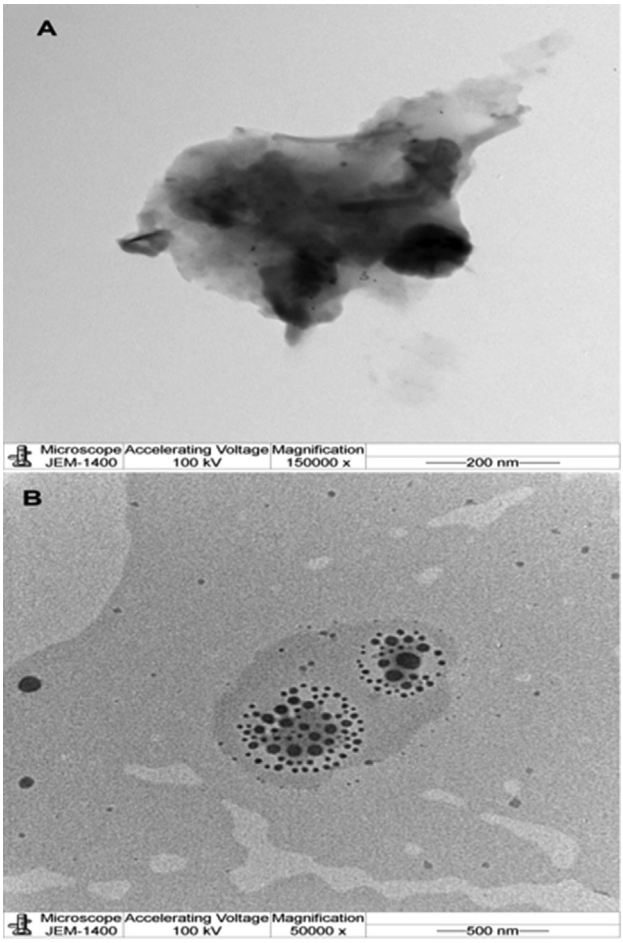

Fig. 5. TEM photographs of (A) FLZ nanoparticle (F3) and (B sodium alginate gel formulation containing FLZ nanoparticle (F3).

the Zetasizer was 352 ± 6.1 nm while that obtained with TEM was around 400 nm. Fig. 5 (B) shows the TEM image of sodium alginate gel containing FLZ nanoparticle formulation (F3), where the size of the FLZ nanoparticle was also about 400 nm.

3.2.5. In vitro drug release study

The *in vitro* release of FLZ from the nanoparticle gel formulations containing two different polymers, carbopol 934 and sodium alginate, in two concentrations (1 and 3% w/w) was examined as given in Table 2. The obtained results indicated that the release rate of FLZ from these nanoparticle gel formulations were significant ($P < 0.05$) compared to that from the untreated formulation (F0). Based on Table 2, at 1% w/w carbopol 934, the percent amount of drug released after 6 h was 100 ± 0.0, 101.3 ± 2.3, and 100 ± 0.0 for F3, F4, and F13, respectively, while that from F0 was 44.9 ± 4.0. The enhanced *in vitro* release rates of FLZ nanoparticles from gel formulations in comparison to the untreated drug might be due to the reduction of drug particle size, in addition to the penetration enhancing effect of the stabilizers used. El-Feky et al. showed that increase permeation rate of Acylovir nanosuspension through cellophane membrane was due to enlarged surface area of the nanosuspension formula, in addition to, the solubilizing effects of nanoparticles stabilizers; Pluroinc® F68 and tween® 80.

Although the F3 formulation had a higher viscosity (4.998 ± 0.5 Pa.s) than F0 (1.926 ± 0.17 Pa.s), the release rate of the drug from F3 was 100 ± 0.0 while that from F0 was 44.9 ± 4.0. The higher release rate of the F3 formulation may be due to the surfactant nature of PL F 127, which was employed in the F3 formula. The solubility of the drug (2.8 ± 0.808 mmol/L) increased by means of PL F 127 comparative to that of F0 (1.2 ± 0.215 mmol/L). For F4, the higher percentage of the drug released relative to the untreated drug F0 might be due to its low viscosity relative to F0 (1.266 ± 0.27 and 1.926 ± 0.17, respectively). F4 also had a higher solubility of 5.2 ± 1.418 mmol/L than F0. The lower viscosity and higher solubility of F13 directed to an improve in the release rate of FLZ. F13 had a viscosity of 0.766 ± 0.02 Pa.s at the 20 s^{-1} shear rate. Although the viscosity of F7 was higher than that of F0, the release rate of FLZ was also higher (56.6 ± 0.0) in F7. F11 had the same percentage of FLZ release relative to the untreated drug F0, which may be due to the similar viscosity between the two formulas. The higher release rate of F16 may be due the lower gel viscosity (1.8 26 ± 0.28 Pa.s).

The *in vitro* release rate of FLZ from the nanoparticle gel formulation comprising sodium alginate (F0) was 32.8% ±1.1 after 6 h as shown in Table 2. The release rate of the F11 formulation containing xanthan gum and the F13 containing PVP showed slight decreases of 30.5 ± 2.3 and 30.3 ± 3.7, respectively, which can be attributed to their similar viscosity to F0. The formulations F3 (42.4 ± 3.6), F4 (45.5 ± 5.2), and F7 (37.8 ± 5.5) had an increase in their release compared to F0 (32.8 ± 1.1) which might be due to their increased solubility compared to F0 (2.8 ± 0.808, 5.2 ± 1.418, 3.3 ± 0.332, and 1.2 ± 0.215 mmol/mL, respectively). F16 had the highest release of FLZ (63.8 ± 0.0); this might be explained by the SLS surfactant characteristic, which lowers the surface tension, thereby promoting the adequate release of the nanoparticle from the sodium alginate gel formulation (Shid et al, 2014). To find out the release mechanism that suitable depicts the model of drug release, the *in vitro* release records were tested using the zero order, first order, Higuchi diffusion model, and Korsmeyer-Peppas model. The mechanism of drug release followed the Higuchi diffusion model consistent with the highest obtained correlation coefficient displayed in Table 3. The value of n is used to define whether the diffusion mechanism is Fickian diffusion ($n < 0.5$), anomalous diffusion (non-Fickian) ($0.5 < n < 1$), or near zero order release ($n = 1$). As shown in Table 3, most formulations had an n (release exponent) value < 0.5, thereby revealing the Fickian diffusion model. For the F3 and F4 carbopol gel and the F7 and F16 sodium alginate gel the non-Fickian diffusion mechanism was detected.

Table 2
In vitro release of FLZ from different nanoparticles carbopol and sodium alginate gel formulations (n = 3, mean ± SD).

Formula	% FLZ cumulative released after 6 h	
	Carbopol 934 gels	Sodium alginate gels
F0*	44.9 ± 4.0	32.8 ± 1.1
F3	100 ± 0.0	42.4 ± 3.6
F4	100.3 ± 2.3	45.5 ± 5.2
F7	56.6 ± 0.0	37.8 ± 5.5
F11	45.4 ± 7.1	30.5 ± 2.3
F13	100 ± 0.0	30.3 ± 3.7
F16	54.4 ± 2.8	63.8 ± 0.0

* **F0:** untreated FLZ

3.2.6. Ex vivo permeation study

Ex vivo transcorneal permeation studies were carried out to compare the corneal permeation of the gel formulations containing FLZ nanoparticle formula that showed highest *in vitro* release from cellophane membrane (F3) with gel containing untreated drug. The selected formulations had significantly higher permeation throughout the freshly excised goat cornea than F0. In particular, after 8 h, sodium alginate gel containing the FLZ nanoparticle formulations had a significant increase in the percent of drug permeation relative to F0. The percent of drug permeation from alginate gel containing F3 nanoparticle formula was 100.3 ± 7.8 while that from F0 was 64.1 ± 2.3 after 8 h (Fig. 6). In addition, the F3-loaded alginate gel formulation had a significantly lower viscosity (0.484 ± 0.11 Pa.s) than F0 (1.926 ± 0.17 Pa.s). The higher percent of drug penetration from the gel containing F3 nanoparticle formula might be also due the small particle size (352 ± 6.1 nm) of F3 nanoparticles with high zeta potential value (-18.3 mV), which caused enhanced transcorneal permeation (De Campos et al, 2001; Abdellatif et al, 2019). In addition, the surfactant nature of PL F 127 might additionally result in enhanced transcorneal drug permeation (Mandal et al, 2017).

The permeation parameters of FLZ, the steady state fluxes (J_{ss}) and permeability coefficients (P), were calculated from the *ex vivo* permeation data across the goat corneal membrane. The steady state diffusion was calculated using:

$J_{ss} = - D\ dC/dx$

Where dC/dx is the gradient of the concentration C, and D is the diffusion constant. The permeation coefficient (P; the velocity of drug passage through the membrane in cm/h) was calculated with the equation: $P = J_{ss}/C_o$, where P is the permeation coefficient, Jss is the flux, and C_o is the concentration of the donor solution (Dinesh, 2016).

The permeation parameters of FLZ from the different nanoparticles loaded in the carbopol and sodium alginate gel across the goat cornea are listed in Table 4. All formulations were found to have higher drug flux (J_{ss}) and permeation coefficient (kp) than F0. In fact, the flux values ranged from 19.39 ± 2.0 to 31.9 ± 3.9 μg/cm^2/h for the carbopol nanoparticle gel compared to the 20.9 ± 2 μg/cm^2/h obtained for F0. The same finding was obtained for the permeability coefficient values, with the highest permeability coefficient value (6.3 ± 3.9 cm/h x10^3) obtained with F3. The FLZ nanoparticle formulas having sodium alginate, F3 and F4, had a significant enhance in drug flux compared to F0 as shown in Table 4. The permeation parameters of FLZ from F3 nanoparticle formula from sodium alginate gel base was significantly higher than from carbopol gel, in which the computed flux value was 148.54 ± 2.6 5 μg/cm^2/h with a permeability coefficient of 29.71 ± 2.65 cm/h

Table 3
The kinetic parameters of the *in vitro* release of FLZ from carbopol 934 and sodium alginate gel formulations containing drug nanoparticles.

Formula	Carbopol 934 gels			Sodium alginate gels		
	Linear regression analysis using correlation coefficient R^2 according to					
	Higuchi	Korsmeyer-Peppas		Higuchi	Korsmeyer-Peppas	
		R^2	n		R^2	n
F0	0.883	0.730	0.322	0.929	0.741	0.185
F3	0.948	0.888	0.780	0.980	0.966	0.305
F4	0.910	0.832	0.668	0.979	0.938	0.287
F7	0.964	0.925	0.410	0.883	0.293	0.503
F11	0.947	0.771	0.347	0.936	0.729	0.272
F13	0.978	0.940	0.467	0.985	0.995	0.328
F16	0.920	0.614	0.206	0.960	0.911	0.609

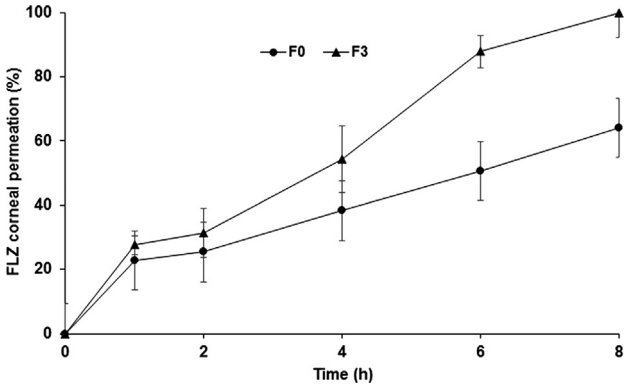

Fig. 6. *Ex-vivo* transcorneal permeation of FLZ nanoparticle formula (F3) from sodium alginate ocular gel compared to the untreated drug (n = 3, mean ± SD).

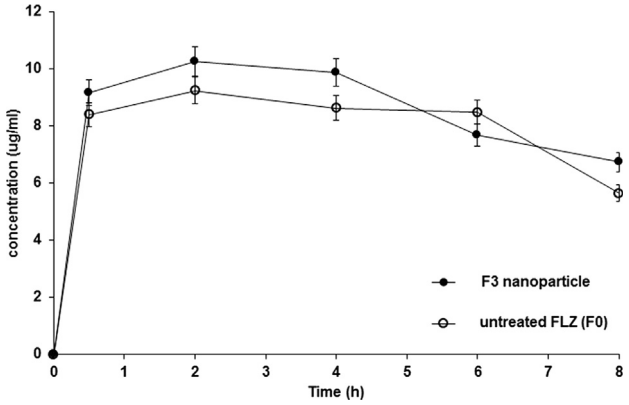

Fig. 7. Concentration-time curve of FLZ from sodium alginate ocular gel containing its nanoparticle formula (F3) compared to sodium alginate ocular containing the untreated drug (F0). Results (n = 3) are presented as (mean ± SD).

x10^3. These nanoparticles also had the highest permeability coefficient values compared to F0. Therefore, sodium alginate gel base containing F3 nanoparticles formula will be selected for *in vivo* performance for ocular pharmacokinetics.

3.2.7. In vivo performance of the FLZ nanoparticles in the ocular gel

After the topical ocular application of the sodium alginate gel containing the selected nanoparticle formula, F3, and untreated FLZ to the eyes of the rabbit, the mean aqueous humor concentration as a function of time was calculated. The pharmacokinetic parameters of both formulations are presented in Fig. 7 and Table 5. As time progressed, the aqueous humor concentration was found to increase and reach maximum peak after two h for both formulae (T_{max}). The results revealed that the C_{max} of FLZ in F0 (10.25 ± 3. 86 ng/mL) was slightly but not significantly higher than that in F3 (9.72 ± 3.64 ng/mL); according to the statistical analysis, there was no significant difference ($P > 0.05$) between the C_{max} of the two formulations. After the second hour, the gel formula containing the untreated FLZ (F0) was rapidly eliminated (K = 1.09 ± 0.4 5 h^{-1}) relative to that containing nanoparticle formula (F3) (K = 0.406 ± 0.103 h^{-1}), with the former exhibiting a 2.7-fold greater K than the latter ($P < 0.0001$). F3 also had a longer elimination half-life (1.71 h) than F0 (0.636 h). Furthermore, the $AUC_{0\text{-}8h}$

Table 5
Pharmacokinetic parameters for FLZ following an ocular application of sodium alginate gel containing its nanoparticle formula (F3) compared to gel containing the untreated drug (F0) in rabbit aqueous humor.

Pharmacokinetic Parameters	Ocular gel containing untreated drug (F0)	Ocular gel containing nanoparticle formula (F3)
C_{max} (ng/ml)	10.25 ± 3.86	9.72 ± 3.74
T_{max} (h)	2 ± 0.02	2 ± 0.06
K (h^{-1})	1.09 ± 0.45	0.41 ± 0.10 *
$t_{1/2}$ (h)	0.64 ± 0.45	1.71 ± 0.10
$AUC_{0\text{-}8}$(ng/ml. h^{-1})	9.68 ± 0.99	13.18 ± 0.54 **

* P < 0.0001,
** P = 0.0057

Table 4
Ex vivo permeation parameters of FLZ from different nanoparticles gel formulations (n = 3, mean ± SD).

Nanoparticle Formula	Carbopol 934 gel		Sodium alginate gel	
	Flux (Jss) (μg/cm2h^{-1})	Permeability coefficient (kp) (cm/h) x10^3	Flux (J_{ss}) (μg/cm2h^{-1})	Permeability coefficient (kp) (cm/h) x10^3
F0	20.9 ± 2.00	4.2 ± 2.00	125.73 ± 5.20	25.1 ± 5.2
F3	31.90 ± 3.90	6.3 ± 3.90	148.54 ± 2.65	29.71 ± 2.65
F4	24.77 ± 7.25	4.9 ± 7.25	171.46 ± 2.90	34.3 ± 2.90
F7	19.39 ± 2.00	3.8 ± 2.00	98.43 ± 5.40	19.7 ± 5.40
F11	23.88 ± 1.63	4.8 ± 1.63	86.33 ± 6.35	17.3 ± 6.35
F13	26.37 ± 1.87	5.2 ± 1.87	74.06 ± 3.50	14.8 ± 3.50
F16	28.22 ± 2.80	5.6 ± 2.80	115.02 ± 2.42	23.01 ± 2.42

recorded after the ocular application of the sodium alginate gel containing the FLZ nanoparticle (F3) was significantly (P = 0.0057) higher (1.4-fold) than that of the gel bases containing the untreated drug; the $AUC_{0\text{-}8h}$ of F3 and F0 was 13.18 ± 0.84 and 9.68 ± 0.99 ng/mL/h, respectively. Such findings might indicate the higher extent of drug release and the higher bioavailability of FLZ from the selected nanoparticle formula. Compared to the gel containing the untreated drug, that containing the FLZ nanoparticle could reside in the eye of rabbits for a specific period, enabling FLZ release, with increases in the AUC and t½.

4. Conclusion

Based on the findings obtained herein, application of solvent precipitation techniques was useful to obtain FLZ nanoparticles of small sizes with small PDI values, especially in case of using 5% of the stabilizers used. In addition, a correlation exists between the *in vitro* and *ex vivo* release of FLZ and the *in vivo* transcorneal drug permeation. Aqueous humor concentration from gel base loaded with nanoparticle formula (F3) was significantly improved when compared to that with untreated drug (F0).

The introduction of FLZ nanoparticles to the ophthalmic gel formulations can improve the characteristic of the drug release of the small nanoparticles from the gel vehicles and enhance drug permeation through the cornea, in addition to minimizing drug corneal irritating effect. Moreover, incorporating the nanonized drug particles in a gel base may increase corneal residence time that can result in increasing its ocular bioavailability.

Acknowledgements

The authors extend thier appreciation to the Deanship of Scientific Research at King Saud University for funding the work through the Research Group number RG-1440-035.

References

Abbasoglu, Ö.E., Hoşal, B.M., Şener, B., Erdemoglu, N., Gürsel, E., 2001. Penetration of topical fluconazole into human aqueous humor. Exp. Eye Res. 72, 147–151.
Abdellatif, A.A.H., El-Telbany, D.F.A., Zayed, G., Al-Sawahli, M.M., 2019. Hydrogel Containing PEG-Coated Fluconazole Nanoparticles with Enhanced Solubility and Antifungal Activity. J. Pharm. Innov. 14, 112–122.
Abou el Ela, A.E.S.F., El Khatib, M.M., 2014. Formulation and evaluation of new long acting metoprolol tartrate ophthalmic gels. Saudi Pharm. J. 22, 555–563.
Abou el Ela, A.E.S.F., El Khatib, M.M., Salem-Bekhit, M.M., 2017. Design, characterization and microbiological evaluation of microemulsion based gel of griseofulvin for topical delivery system. Biointerface Res. Appl. Chem. 7, 2277–2285.
Alshora, D.H., Alsaifa, S., Ibrahima, M.A., Ezzeldinc, E., Almeanazel, O.T., El Ela, A.E.F., Ashri, L.Y., 2020. Co-stabilization of pioglitazone HCL nanoparticles prepared by planetary ball milling: *in-vitro* and in-vivo evaluation. Pharm. Dev. Technol. 25 (7), 845–854.
Alshora, D.H., Ibrahim, M.A., Elzayat, E., Almeanazel, O.T., Alanazi, F., 2018. Rosuvastatin calcium nanoparticles: Improving bioavailability by formulation and stabilization codesign. PLoS ONE. 13, E200–E218.
Behrens-Baumann, W., Klinge, B., Rüchel, R., 1990. Topical fluconazole for experimental candida keratitis in rabbits. British J. Ophthalmol. 74, 40–42.
Chen, H., Khemtong, C., Yang, X., Chang, X., Gao, J., 2011. Nanonization strategies for poorly water-soluble drugs. Drug Discov. Today 16, 354–360.
De Campos, A.M., Sanchez, A., Alonso, M.J., 2001. Chitosan nanoparticles: a new vehicle for the improvement of the delivery of drugs to the ocular surface: Application to cyclosporin A. Int. J. Pharm. 224, 159–168.
Dinesh, B., 2016. Effect of permeation enhancers on permeation kinetics of midazolam, *in-vitro* characterization. Asian J. Pharm. 1, 55–62.
El-Feky, G.S., Zayed, G., Farrag. 2013. Optimization of an ocular nanosuspension formulation for acyclovir using factorial design. Int. J. Pharm. Pharm. Sci. 5, 213-219.
El-Kamel, A.H., 2002. *In vitro* and *in vivo* evaluation of Pluronic F127-based ocular delivery system for timolol maleate. Int. J. Pharm. 24, 47–55.
Gao, L., Zhang, D., Chen, M., 2008. Drug nanocrystals for the formulation of poorly soluble drugs and its application as a potential drug delivery system. J. Nanopart. Res. 10, 845–862.
Gonjari, I.D., Hosmani, A.H., Karmarkar, A.B., Godage, A.S., Kadam, S.B., Dhabale, B.N., 2009. Formulation and evaluation of in situ gelling thermoreversible mucoadhesive gel of fluconazole. Drug Discov. Ther. 3 (1), 6–9.
Habib, F.S., Fouad, E.A., Abdel-Rhaman, M.S., Fathalla, D., 2010. Liposomes as an ocular delivery system of fluconazole: *in-vitro* studies. Acta Ophthalmol. 88, 901–904.
Hornof, M., Toropainen, E., Urtti, A., 2005. Cell culture models of the ocular barriers. Eur. J. Pharm. Biopharm. 60, 207–225.
Ibrahim, M.A., 2014. Tenoxicam-Kollicoat IR® Binary Systems: Physicochemical and Biological Evaluation. Acta Pol. Pharm. Drug Research 71 (4), 647–659.
Ibrahim, M.A., Shazly, G.A., Aleanizy, F.S., Alqahtani, F.Y., Elosaily, G.R., 2019. Formulation and Evaluation of Docetaxel Nanosuspensions: *In-vitro* Evaluation and Cytotoxicity. Saudi Pharm. J. 27, 49–55.
Junghanns, J.U.A., Müller, R.H., 2008. Nanocrystal technology, drug delivery and clinical applications. Int. J. Nanomed. 3, 295–309.
Keck, C.M., Müller, R.H., 2006. Drug nanocrystals of poorly soluble drugs produced by high pressure homogenisation. Eur. J. Pharm. Biopharm. 62, 3–16.
Mandal, A., Bisht, R., Rupenthal, I.D., Mitra, A.K., 2017. Polymeric micelles for ocular drug delivery: From structural frameworks to recent preclinical studies. J. Control. Release. 28 (248), 96–116.
Marcato, P.D., Durán, N., 2008. New aspects of nanopharmaceutical delivery systems. J. Nanosci. Nanotechnol. 8, 2216–2229.
Merisko-Liversidge, E., Liversidge, G.G., Cooper, E.R., 2003. Nanosizing: a formulation approach for poorly-water-soluble compounds. Eur. J. Pharm. Sci. 18, 113–120.
Pathak, M.K., Chhabra, C., Pathak, K., 2013. Design and development of a novel pH triggered nanoemulsified in-situ ophthalmic gel of fluconazole: Ex-vivo transcorneal permeation, corneal toxicity and irritation testing. Drug Dev. Ind. Pharm. 39 (5), 780–790.
Paun, J., Tank, H., 2012. Nanosuspension: An emerging trend for bioavailability enhancement of poorly soluble drugs. Asian. J. Pharm. Technol. 2, 157–168.
Sayed, E.G., Hussein, A.K., Khaled, K.A., Ahmed, O.A., 2015. Improved corneal bioavailability of ofloxacin: biodegradable microsphere-loaded ion-activated in situ gel delivery system. Drug Des. Devel. Ther. 9, 1427–1435.
Shid, R.L., Dhole, S.N., Kulkarni, N., Shid, S.L., 2014. Formulation and evaluation of nanosuspension delivery system for simvastatin. Int. J. Pharm. Sci. Nanotechnol. 7, 2459–2476.
Van Eerdenbrugh, B., Van den Mooter, G., Augustijns, P., 2008. Top-down production of drug nanocrystals: nanosuspension stabilization, miniaturization and transformation into solid products. Int. J. Pharm. 264, 64–75.
Wadhwa, S., Paliwal, R., Paliwal, S.R., Vyas, S., 2009. Nanocarriers in ocular drug delivery: an update review. Current Pharm. Des. 15, 2724–2750.
Xue, D., Sethi, R., 2012. Viscoelastic gels of guar and xanthan gum mixtures provide long-term stabilization of iron micro-and nanoparticles. J. Nanopart. Res. 14, 1239–1253.
Zaki, R., Hosny, K.M., Abd-elbary, A., 2011. Ketorolac tromethamine in-situ ocular hydro gel; preparation, characterization, and *in-vivo* evaluation. Int. J. Drug Deliv. 3, 535–545.
Zimmer, A., Kreuter, J., 1995. Microspheres and nanoparticles used in ocular delivery systems. Adv. Drug Deliv. Rev. 16, 61–73.